TISSUE-SPECIFIC PROGENITOR AND STEM CELLS

STEM CELLS
TRANSLATIONAL MEDICINE

Role of extracellular vesicles from adipose tissue- and bone marrow-mesenchymal stromal cells in endothelial proliferation and chondrogenesis

Cansu Gorgun[1,2] 🄸 | Maria Elisabetta Federica Palamà[1] 🄸 | Daniele Reverberi[3] |
Maria Cristina Gagliani[1] | Katia Cortese[1] | Roberta Tasso[1] | Chiara Gentili[1] 🄸

[1]Department of Experimental Medicine
(DIMES), University of Genova, Genoa, Italy

[2]U.O. Cellular Oncology, IRCCS Ospedale
Policlinico San Martino, Genoa, Italy

[3]U.O. Molecular Pathology, IRCCS Ospedale
Policlinico San Martino, Genoa, Italy

Correspondence
Roberta Tasso, PhD and Chiara Gentili, PhD,
Department of Experimental Medicine,
University of Genova, 16132, Genoa, Italy.
Email: roberta.tasso@unige.it (R.T.) and chiara.
gentili@unige.it (C.G.)

Funding information
Marie Sklodowska—Curie, Grant/Award
Number: 721432 CarBon; European Union's
Horizon 2020, Grant/Award Number: 874671

Abstract

The secretome of mesenchymal stromal cells (MSCs) derived from different tissue sources is considered an innovative therapeutic tool for regenerative medicine. Although adipose tissue-and bone marrow-derived MSCs (ADSCs and BMSCs, respectively) share many biological features, the different tissue origins can be mirrored by variations in their secretory profile, and in particular in the secreted extracellular vesicles (EVs). In this study, we carried out a detailed and comparative characterization of middle- and small-sized EVs (mEVs and sEVs, respectively) released by either ADSCs or BMSCs. Their involvement in an endochondral ossification setting was investigated using ex vivo metatarsal culture models that allowed to explore both blood vessel sprouting and bone growth plate dynamics. Although EVs separated from both cell sources presented similar characteristics in terms of size, concentration, and marker expression, they exhibited different characteristics in terms of protein content and functional effects. ADSC-EVs overexpressed pro-angiogenic factors in comparison to the BMSC-counterpart, and, consequently, they were able to induce a significant increase in endothelial cord outgrowth. On the other hand, BMSC-EVs contained a higher amount of pro-differentiation and chemotactic proteins, and they were able to prompt growth plate organization. The present study highlights the importance of selecting the appropriate cell source of EVs for targeted therapeutic applications.

KEYWORDS
cartilage and bone development, ex vivo metatarsal culture model, extracellular vesicles, mesenchymal stromal cells, regenerative medicine

SIGNIFICANCE STATEMENT
Mesenchymal stromal cells are a great source for regenerative medicine applications. Cells derived from different tissues might have distinctive characteristics. Many

---

---

studies suggest a critical therapeutic role for extracellular vesicles secreted by stromal cells. The authors characterized extracellular vesicles isolated from two different sources (bone marrow, adipose tissue). Despite, minimal structural differences, the authors observed different functional effects during the differentiation and maturation of cartilage tissue. Therefore, a deep investigation of biological effects is essential before selecting the optimal extracellular vesicle-cell source to be used in specific therapeutic settings.

1 | INTRODUCTION

A combination of regenerative and trophic properties has prompted exploration of the therapeutic use of mesenchymal stromal cells (MSCs) over the last decades.[1] MSCs virtually reside in all tissues, where part of them localize near the microvasculature walls, stabilizing endothelial networks.[2,3] Thanks to manifold mechanisms through which MSCs act, they are considered a powerful tool for the treatment of various diseases.[4] Although bone marrow (BM) has been regarded as the gold standard source, it presents significant drawbacks, such as low cell yield and invasive and painful procedure for BM collection.[5] These issues induced the scientific community to analyze and characterize MSCs from alternative sources.[6] Among the others, adipose tissue (AD) represents a promising source for its abundance, accessibility and less invasive collection.[7] Although MSCs from different tissues share many biological features, some differences exist in the immunophenotype, proliferative capacity, differentiation potential, gene expression profile and immunomodulatory activity.[8,9] Altogether, these putative disparities can lead to different efficacies. For example, it has been reported that ADSCs possess a higher angiogenic potential in comparison to bone marrow-MSCs (BMSCs).[10] Therefore, there may be the advantage of using a cell population over another for specific clinical applications.

Apart from differentiation potential, it is now accepted that MSCs exert their beneficial effects promoting cytoprotection and tissue repair through their paracrine activity.[11] Among the components responsible for the paracrine effects, extracellular vesicles (EVs) have been recently described as new players in cell-cell communication and tissue homeostasis.[12] EVs are a heterogeneous group of cell-derived membranous structures comprising small-sized vesicles (exosomes) originating from the endosomal compartment and middle-sized vesicles (microvesicles) directly budding from the cell plasma membrane.[13] MSC-derived EVs are involved in a wide spread of processes, including angiogenesis, senescence, proliferation, and differentiation, beside strong immunomodulatory properties.[14] Since EVs trigger specific cellular responses, reflecting the status and composition of the parental cell, we here aimed to identify morphological and functional differences between BMSC- and ADSC-derived EV subpopulations. EVs were isolated from the cell conditioned media by serial differential centrifugations, to collect both medium-sized and small-sized vesicles. The role of EVs in the different phases of the endochondral ossification (EO) process, namely angiogenesis, chondrogenic, and osteogenic differentiation, was evaluated taking advantage of fetal mouse metatarsal bone explants.

Just as in some pathologies there may be the advantage of using one cell population over another, in the same way it may be important to know in depth the functional differences between the corresponding EVs to be used in cell-free therapeutic approaches.

2 | METHODS

2.1 | Isolation and culture of MSCs

Human ADSCs were obtained from subcutaneous AD, isolated and cultured, as previously described,[15] and in compliance to Regione Liguria Ethical Committee authorization (P.R. 23571). Human BMSCs were obtained from femoral condyles of patients undergoing knee arthroplasty, after informed consent and according to the guidelines of the Ethics Committee of IRCCS Policlinico San Martino Hospital (Genoa, Italy), N. Registro CER Liguria: 372/2019. For more details, please see Supplemental Materials.

2.2 | EVs separation and characterization

We have submitted all relevant data of our experiments to the EV-TRACK knowledgebase (EV-TRACK ID: EV210113).[16] When ADSCs and BMSCs reached 70% confluence, they were rinsed twice with PBS and maintained for 20 minutes in culture medium without FBS (serum-free medium). Medium was then replaced with fresh serum-free medium, and cells were maintained for 24 hours in starvation. Cell conditioned media (CM) were collected and centrifuged at 300g for 10 minutes and at 2000g for 20 minutes to remove cells/cell debris and apoptotic bodies. Supernatants were transferred into ultracentrifugation tubes (Beckman-Coulter) and subjected to a first centrifugation at 10 000g for 40 minutes to obtain an EV pellet (10 K pellet) enriched in medium sized-vesicles (mEVs). Resulting supernatants were then centrifuged at 100 000g for 120 minutes in order to obtain a pellet (100 K pellet) enriched

in small sized-vesicles (sEVs).[17] Both EV pellets were washed in PBS and centrifuged at 100 000*g*. A Beckman Coulter ultracentrifuge (Beckman Coulter Optima XPN-100 ultracentrifuge; Beckman Coulter) was used with the swinging bucket rotors SW28 and SW55Ti. After the last washing step, EVs were resuspended in sterile filtered (0.22 μm) PBS for further analysis. The concentration of membrane-bound proteins on the surface of freshly isolated EVs was measured by BCA (bicinchoninic acid) Protein Assay Kit (Thermo Fisher Scientific, Massachusetts).

EV concentration and size distribution were analyzed by tunable resistive pulse sensing (TRPS).[18] Imaging of cells and corresponding EVs were performed by trasmission electon microscopy (TEM). Isolated mEVs and sEVs from ADSCs and BMSCs were analyzed by western blot[19] and nonconventional flow cytometry.[20] For more details, please see Supplemental Materials.

2.3 | Cytokine and chemokines arrays

For the analysis of cytokine and chemokine content of EVs, 10 μg of proteins were analyzed with a Proteome Profiler Human XL Cytokine Array Kit (R&D, Minneapolis, Toll Free USA, Canada), according to the manufacturer's instructions. Images were scanned using the Epson perfection 1260 scanner and spot densities were quantified using the ImageJ software. Gene Ontology (GO) was also carried out using DAVID.

2.4 | Ex vivo metatarsal sprouting assay

All animal procedures were approved by the Italian Ministry of Health, by the IRCCS Ospedale Policlinico San Martino Ethical Committee (Authorization n. 55/2020-PR) and performed in accordance with the national current regulations regarding the protection of animals used for scientific purpose.

E17.5 fetuses were removed from pregnant C57BL/6 wild-type mice and metatarsals were dissected under stereomicroscope. The isolated metatarsals were cultured in 24-well plates in 300 μL of α-MEM-GlutaMAX medium (Gibco, Waltham, Massachusetts), supplemented with 10% FBS (Gibco, Milan, Italy) and 50 mg/mL penicillin/streptomycin for 96 hours. After 96 hours, attached bones covered with fibroblasts were selected and medium was replaced with α-MEM-GlutaMAX supplemented with 2% FBS. For each replicate, experimental groups have been set as follows: (a) negative control: serum-free α-MEM GlutaMAX; (b) test groups: serum-free α-MEM GlutaMAX supplemented with 0.5 μg of either ADSC-/BMSC-mEVs or ADSC-/BMSC-sEVs; (c) positive control: α-MEM-GlutaMAX supplemented with 10% FBS. After 7 days, bones were analyzed for the expression of CD31 by immunohistochemistry (IHC) and immunofluorescence (IF), as previously described.[21] For more information about IHC and IF, please see Supplemental Materials.

2.5 | Cell proliferation assay

BrDu proliferation assay (cell proliferation enzyme-linked immunosorbent assay (ELISA), bromodeoxyuridine (BrdU), Roche Mannheim, Germany) was performed according to manufacturer's instructions.

2.6 | Ex vivo metatarsal bone growth assay

E15.5 fetuses were removed from pregnant C57BL/6 wild-type mice and metatarsals were dissected under stereomicroscope. The isolated metatarsals were cultured in 24-well plates in 300 μL of α-MEM-GlutaMAX medium, supplemented with 0.2% w/v bovine serum albumin (BSA), 50 mg/mL penicillin/streptomycin and 1× Amphotericin B (basal medium). After 24 hours, 0.5 μg mEVs and sEVs were added. A positive control was used to trigger the bone growth/differentiation by adding 50 μg/mL ascorbic acid, 10 mM β-glycerophosphate and 10^{-7} M dexamethasone (all of them from Sigma-Aldrich, St. Louis, Missouri) to the medium (osteogenic medium). Fresh EVs were added every 3 days, while osteogenic medium was changed every other day in positive controls. Metatarsal cultured in serum-free (basal medium) were used as negative controls. Bone growth was monitored daily and analyzed by Image J software.

2.7 | Histological and immunohistochemical analysis

After 10 days of culture, E15.5 metatarsals were washed with PBS and fixed in 3.7% paraformaldehyde (PFA), then dehydrated and paraffin embedded. Sections of 5 μm were cut, dewaxed, and stained with hematoxylin and eosin (H&E) and Safranin-O/Fast-Green. For more details, please see Supplemental Materials.

2.8 | Statistical analysis

Statistical analysis of differences between multiple groups were performed applying Two-way ANOVA and Tukey's multiple comparisons test. For the analysis of protein arrays, multiple *t* test was performed. Data are presented as mean ± SD considering at least three independent replicates for each assay and analyzed by GraphPad Prism (Graph Pad Software, Inc). For all analyses $P < .05$ was considered statistically significant. In all cases: ****$P < .0001$, ***$P < .001$, **$P < .01$, *$P < .05$.

3 | RESULTS

3.1 | ADSCs and BMSCs release EVs with similar characteristics

Primary cultures of MSCs isolated from either AD or BM have been investigated for their typical mesenchymal phenotype by flow cytometry. According to International Society for Cell

Therapy (ISCT) indications,[22] both ADSCs and BMSCs constitutively expressed the cell surface antigens CD29, CD44, CD73, CD90, and CD105. The expression of CD31, CD34, and CD45 was less than 15%, indicating a poor contamination of endothelial, myeloid, and hematopoietic cells (Supplementary Figure 1A). Only the expression of CD34 by ADSCs was higher than 30%. This is in line with the already published evidence that freshly isolated adipose-derived MSCs (ADSCs) express CD34. Indeed, in these cells CD34 expression disappears after prolonged in vitro culture.[23]

Cell conditioned medium (CM) was collected from either ADSCs or BMSCs maintained for 24 hours in serum free medium. Flow cytometry of Annexin V/PI-stained cells was used to quantify the apoptotic rate of cells exposed to serum deprivation for 24 hours. Less than 1% of both ADSCs and BMSCs underwent apoptosis or necrosis (Supplementary Figure 1B). For EV separation, CM were subjected to differential ultracentrifugation (UC), using an intermediate speed (10 K) prior to a high-speed step (100 K), in order to obtain intermediate recovery and specificity.[24] Material pelleted at 10 K, enriched in medium-sized vesicles (mEVs), was compared with the 100 K pelleted one, considered to be enriched in small-sized EVs (sEVs). Both mEVs and sEVs separated from the two cell sources were firstly characterized by TRPS to check their size and concentration. No significant differences were observed in EV size among the two cell sources (Figure 1A,B). mEVs released by ADSCs and BMSCs exhibited a mean size of 388 ± 32.7 nm and 346 ± 42.1 nm, respectively. sEVs isolated from ADSCs and BMSCs presented a mean size of 138 ± 12 nm and 152 ± 33.2 nm, respectively, indicating that the separation method here adopted allowed the effective and significant separation of two different EV subpopulations (ADSCs: mEVs vs sEVs, $P \leq .0001$; BMSCs: mEVs vs sEVs, $P \leq .001$) (Figure 1A,B). Both cell types released a significantly higher amount of sEVs than mEVs (ADSCs: sEVs vs mEVs, $P < .01$; BMSCs: sEVs vs mEVs, $P < .05$) and with no significant differences between the two cell sources (Figure 1C).

In order to evaluate whether mEVs and sEVs were successfully purified from cells, immunoblotting was performed. Both EV subpopulations, and in particular sEVs isolated from ADSCs and BMSCs expressed the vesicle-associated proteins CD81 and CD63 (Figure 1D). To note, the expression of the tetraspanin CD9 was not detected in any MSC-derived EV. Syntenin, a specific marker for sEVs,[25] was strongly expressed by ADSC- and BMSC-derived sEVs, poorly detected in mEVs and BMSC lysates, and not detected in ADSC lysates (Figure 1D). Interestingly, flotillin-1 was expressed by cell lysates, both mEVs, and by sEVs released only by ADSCs (Figure 1D). As expected, GRP94, a protein of the endoplasmic reticulum used as EV negative marker, was strongly detected only in the cell lysates (Figure 1D). After 24 hours of medium conditioning, isolated EVs, as well as the corresponding MSC monolayers, were analyzed by TEM. Ultrastructural analysis of both cell types revealed the presence of many multivesicular bodies (MVBs) containing several intraluminal vesicles within the cytoplasm, confirming the discharge of a prevalent population of sEVs (Figure 1E, upper panels). The corresponding EV fractions showed the typical round or cup-shaped morphology surrounded by a bilayer membrane, with sizes ranging from 30 to 200 nm (Figure 1E, bottom panels), confirming that the separation procedure picked out a mixed population of vesicles, enriched mostly in sEVs.

ADSC- and BMSC-derived EVs were further characterized for size and marker expression by nonconventional flow cytometry.[20] Both mEVs and sEVs were stained with the cell-permeant, fluorescein-based CFDA-SE tracer, useful to discriminate intact vesicles from debris and membrane fragments. Since CFDA-SE passively diffuses within vesicles and interacts with intra-vesicular enzymes at room temperature (RT) (Figure 2A, bottom panels), 4°C samples were used as controls (Figure 2A, upper panels). Taking advantage of fluorescent dimensional beads (Supplementary Figure 2A), specific size gates were considered (≤100 nm, from 100 to 160 nm and from 160 to 900 nm) (Figure 2B). The percentage of events falling within each dimensional gate was calculated (Supplementary Table 1). While the percentage of vesicles smaller than 100 nm was significantly higher in sEVs released by BMSCs if compared with the mEV counterpart, the percentage of events ranging from 100 and 160 nm, as well as 160 and 900 nm, was significantly higher in BMSC-mEVs compared with sEVs (Supplementary Table 1). A similar trend was also observed in the vesicles released by ADSCs, but no statistically significant differences were detected (Supplementary Table 1). Moreover, no differences were noticed between EVs released by ADSCs and BMSCs, except for the bigger vesicles, ranging from 160 to 900 nm, whose percentage was significantly higher in ADSCs (Supplementary Table 1). Upon accurate titration of antibodies and the use of related isotype controls,[20] the expression of CD81, CD63, and CD9 was evaluated in both mEVs and sEVs (Supplementary Figure 2B,C). All vesicle subpopulations derived from both cell types expressed, at different extent, the three markers. The expression of CD9 was the lowest among the tetraspanins, confirming the western blot analysis. Taken together, these data indicate that MSCs release EV subtypes with similar characteristics, independent of the cell source.

3.2 | Differentially expressed proteins in BMSC- and ADSC-EVs

Although ADSCs and BMSCs share many biological features, little is known about differences in their secreted factors, and in particular EV subtypes. In order to evaluate the protein cargo of both mEVs and sEVs released by ADSCs and BMSCs, vesicle lysates were analyzed using a Proteome Profiler
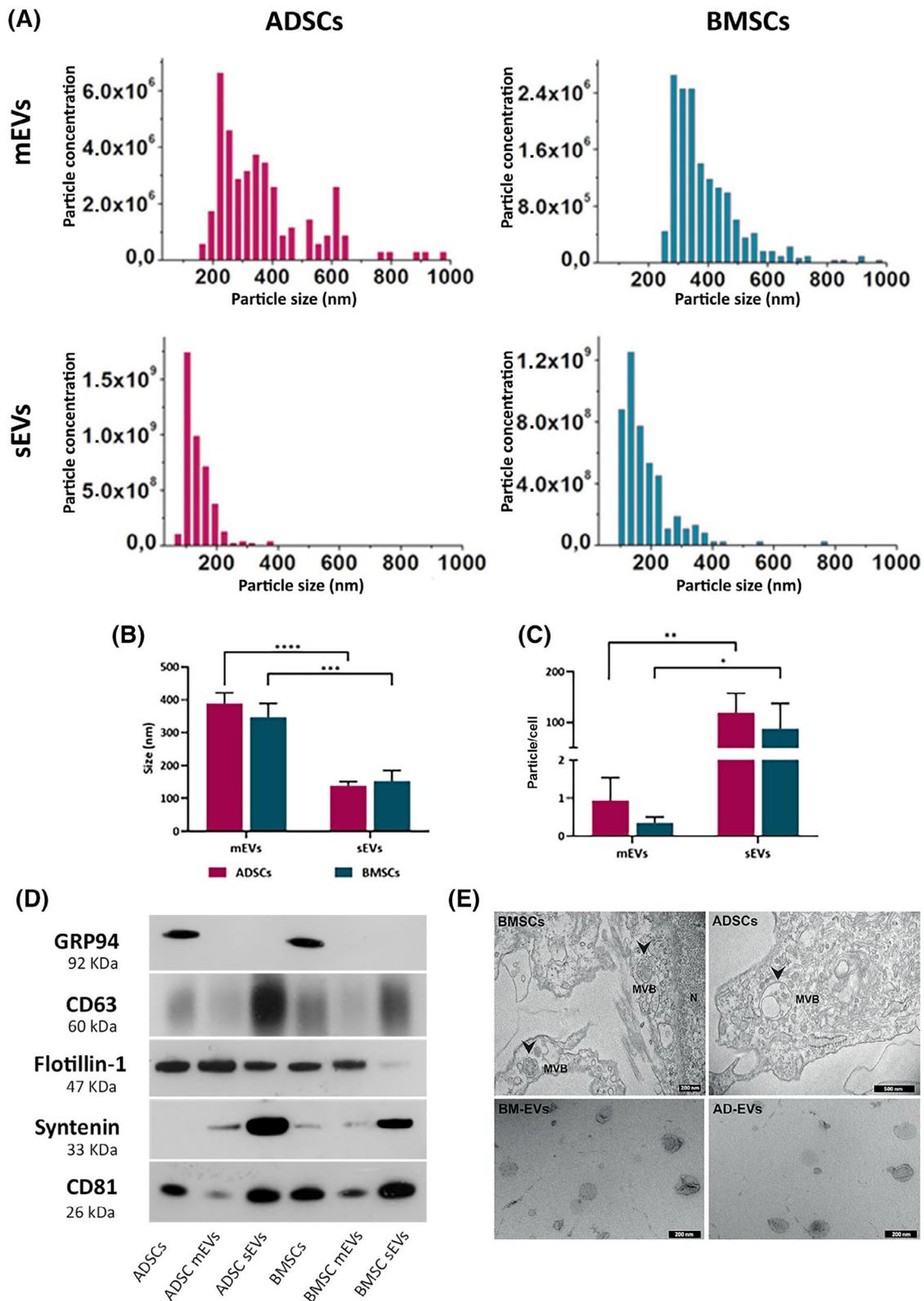
FIGURE 1   ADSCs- and BMSCs-derived EVs have common characteristics. A, Tunable resistive pulse sensing (TRPS) analysis measuring size distribution of ADSC-derived mEVs and sEVs (pink) and BMSC-derived mEVs and sEVs (green). Comparison of size distribution (B), particle counting intended as particle/cell (C). Data are presented as mean ± SD. N = 3, ****$P < .0001$, ***$P < .001$, **$P < .01$, *$P < .05$ (two-way ANOVA and Tukey multiple comparison). D, Western blot analysis on ADSCs and BMSCs-derived mEVs and sEVs. Control cell lysates were also loaded. Specific expressions of CD63, CD81, flotillin, syntenin, and GRP94 were investigated. E, TEM images of preconditioned ADSCs and BMSCs (top panel) and isolated EVs (bottom panel)
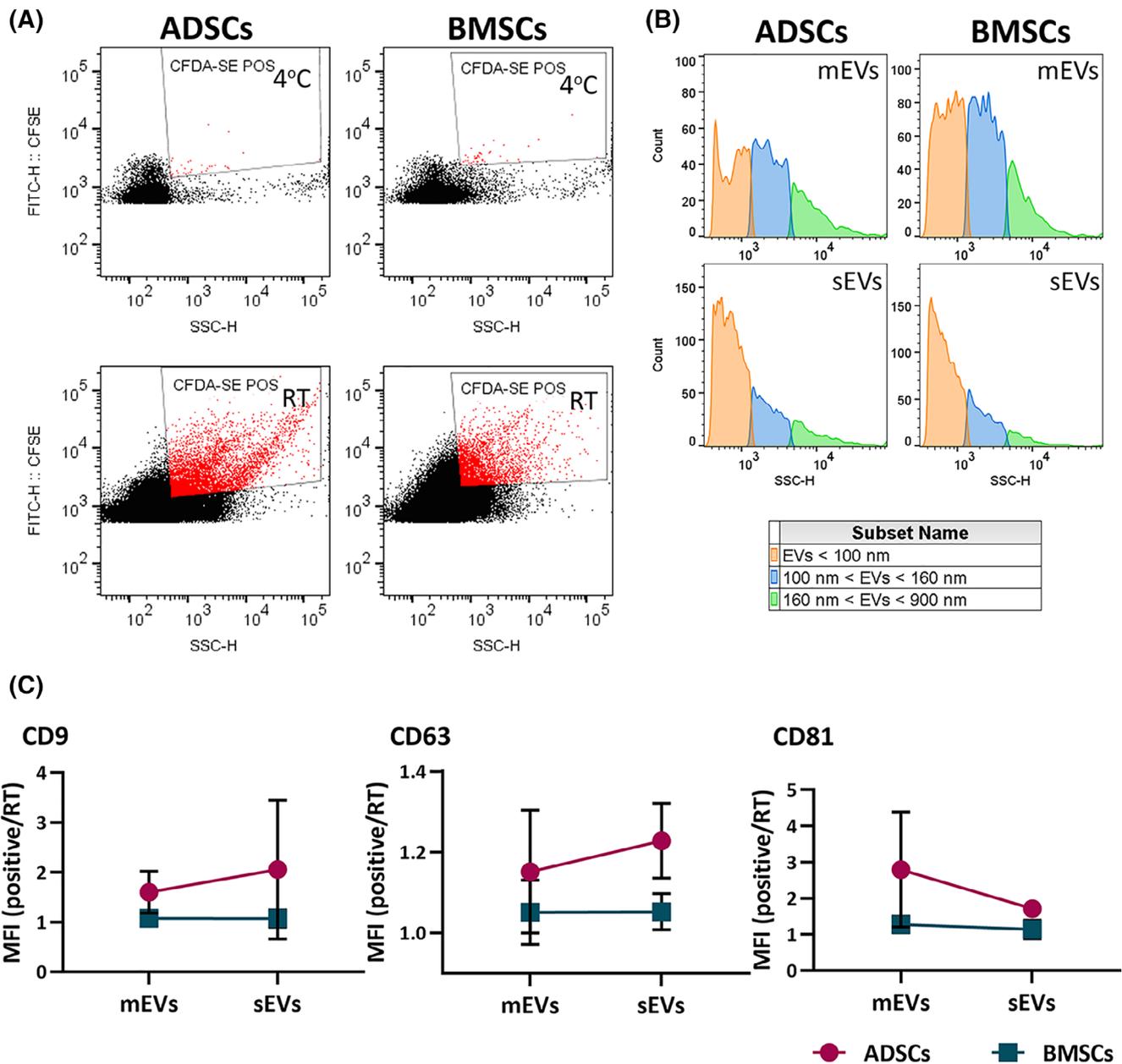
FIGURE 2 Nonconventional flow cytometry strategy used to characterize mEVs and sEVs. A, Red areas identify CFDA-SE positive events. EVs were stained with CFDA-SE at 4°C as "blank tube" (top), useful to define the appropriate dimensional gate when considering EVs stained with CFDA-SE at room temperature (bottom). B, Size distribution of EV subtypes. Three dimensional gates were considered: EVs ≤ 100 nm (orange), 100 nm ≤ EVs ≤ 160 nm (blue), and 160 nm ≤ EVs ≤ 900 nm (green). C, Quantification of CD9-, CD63-, and CD81-positive events falling within the CFDA-SE gate by mEVs and sEVs. Data are presented as ratio between mean fluorescence intensity (MFI) of cells stained with a specific antibody and MFI of correspondent isotype control (relative MFI). Data are representative of at least three independent experiments

optimized to detect cytokines and chemokines (Figure 3). Significant differences were detected not only between mEVs and sEVs derived from the same cell source, but also between the two different cell sources. Gene ontology (GO) analysis was applied to identify key pathways characterizing EV subtypes and the relative frequency of ontology terms (ie, biological functions) was considered. The main biological processes characterizing ADSC- and BMSC-sEVs and mEVs were related to "cell proliferation," "angiogenesis," "regulation of cellular

communication," "defense response," "chemotaxis," "response to external stimulation," and "cell migration," with no significant differences among them (Figure 3A). Supplementary Table 2 resumes the more relevant biological functions and factors involved, with frequency and p value.

Compared with the BMSC-counterpart, ADSC-mEVs presented a significant upregulation of four different proteins, involved, at different extents, in injury environment modulation: DKK-1 (Dickkopf-related protein 1), GRO-α

(A)

Biological processes (mEVs)

Biological processes (sEVs)

ADSCs   BMSCs

(B)
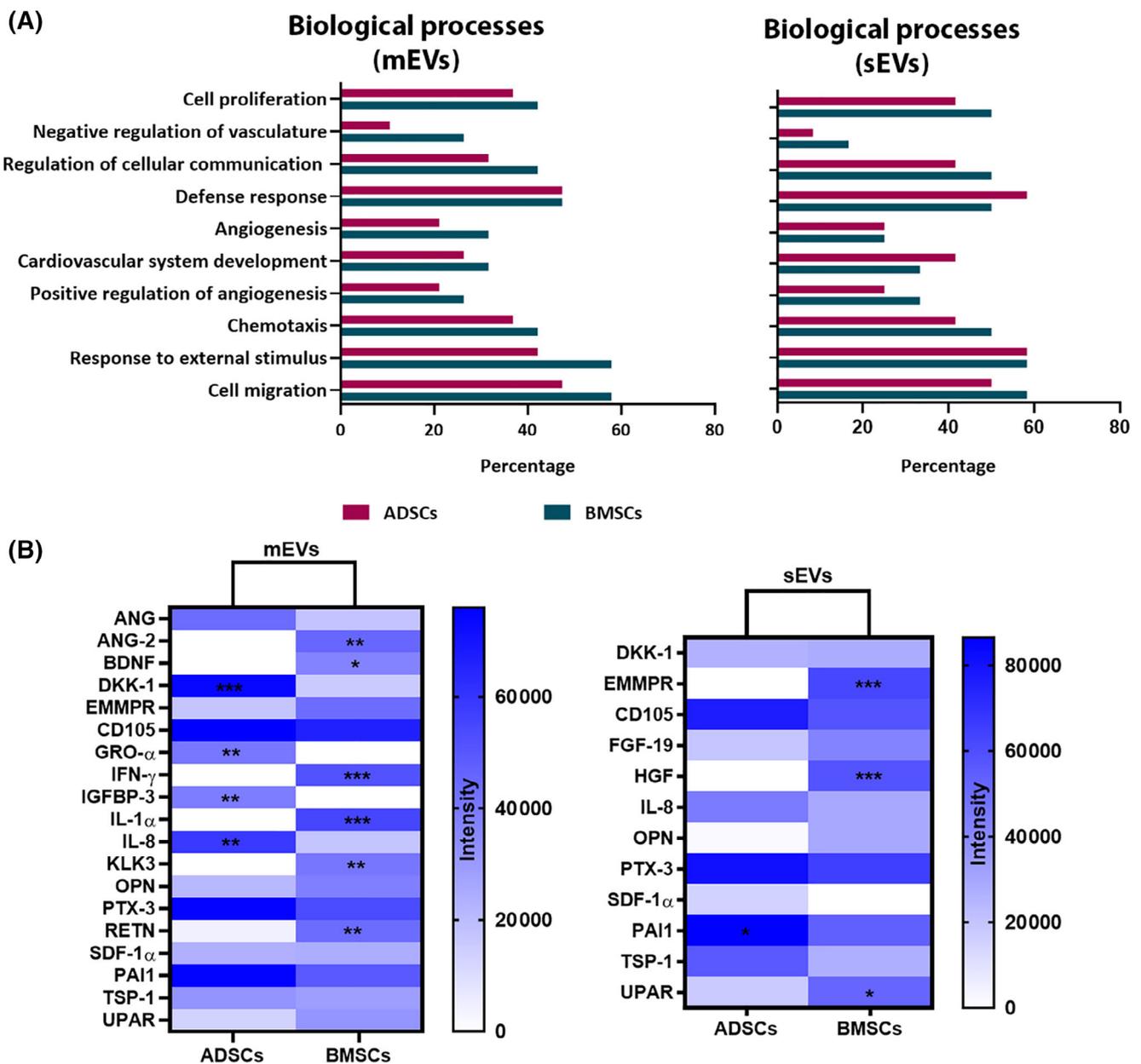
mEVs

sEVs

FIGURE 3 Proteome profiler analysis of ADSC- and BMSC-derived EVs. A, Gene ontology analysis of biological functions in mEVs and sEVs. B, Heatmaps of expressed proteins by mEVs and sEVs. N = 3, (*) presents the statistical differences between the groups. ***$P < .001$, **$P < .01$, *$P < .05$ (multiple t-test comparison). ANG, angiogenin; ANG-2, angiopoietin-2; BDNF, brain-derived neurotrophic factor; DKK1, Dickkopf-1; EMMPRIN, extracellular matrix metalloproteinase inducer; CD105, endoglin; FGF19, fibroblast growth factor 19; GROα, growth-regulated oncogene-alpha; HGF, hepatocyte growth factor; IFNγ, interferon γ; IGFBP3, insulin-like growth factor-binding protein 3; IL1α, interleukin 1 alpha; IL8, interleukin-8; KLK3, kallikrein-3; OPN, osteopontin; PTX3, pentraxin-3; RETN, resistin; SDF1α, stromal cell derived factor 1 alpha; PAI1, plasminogen activator inhibitor-1; TSP1, thrombospondin-1; uPAR, urokinase-type plasminogen activator receptor

(growth-regulated oncogene-alpha), IL-8 (interleukin-8), and IGFBP-3 (insulin-like growth factor binding protein-3) (Figure 3B, left panel). On the contrary, BMSC-derived mEVs exhibited a significant overexpression of proteins involved in the modulation of angiogenic and osteogenic responses (angiopoetin-2 [ANG-2] and brain derived growth factor [BDNF], respectively), as well as in the crosstalk with immune cells (interferon-γ [IFN-γ], interleukin-1α [IL-1α], kallikrein-3 [KLK-3], and resistin [RETN]) (Figure 3B, left panel). Regarding sEVs, only one protein, plasminogen activator inhibitor-1 (PAI-1), was significantly overexpressed by ADSC-derived vesicles (Figure 3B, right panel), while three proteins were significantly upregulated in BMSC-sEVs: EMMPRIN (CD147), hepatocyte growth factor (HGF), and urokinase-type plasminogen activator receptor (uPAR) (Figure 3B, right panel).

3.3 | ADSC-sEVs promote endothelial cord outgrowth from fetal metatarsal explants more efficiently than BMSC-sEVs

We studied the effects of EVs secreted by ADSCs and BMSCs on two different aspects of the EO process. Taking advantage of mouse metatarsal organ explant cultures, E17.5 and E15.5 mice metatarsal were exploited as models of angiogenesis and osteogenesis, respectively.[21,26]

In comparison with other commonly used in vitro or ex vivo angiogenesis assays, endothelial cord outgrowth from mouse fetal metatarsals is more representative of sprouting angiogenesis in vivo.[21] The assay performed on E17.5 metatarsals revealed that ADSC-derived mEVs and sEVs were able to induce the outgrowth of a significant higher number of CD31+ endothelial cords in comparison to BMSC-derived counterparts ($P \leq .05$ and $P \leq .01$, respectively) (Figure 4A,B and Supplementary Figure 3).

Blood vessel formation from metatarsals is the result of complex interactions between various cell types, overall contributing to the development of an intricate vascular network on the top of a fibroblast sheet.[21] Although BMSC-sEVs possessed a lower ability to induce vessel sprouting than ADSC-counterparts, interestingly we noticed a strong induction of

fibroblast proliferation by this experimental group (Figure 4A). This evidence was confirmed by BrdU cell proliferation assay on human umbilical vein endothelial cells (HUVEC) and mouse embryonic fibroblasts (MEFs). Data showed that BMSC-sEVs were able to induce a statistically significant higher HUVEC proliferation in comparison to BMSC-mEVs and ADSC-sEVs ($P < .01$, Figure 4C). BMSC-sEVs also induced a significant increase in MEF proliferation compared with ADSC-counterparts (Figure 4D).

3.4 | Metatarsal bone explants exposed to BMSC-sEVs exhibit more organized growth plate areas compared with ADSC-sEVs

The culture of E15.5 mouse metatarsals is a highly physiological ex vivo model for studying EO and bone growth. Since ADSCs and BMSCs release a significant larger amount of sEVs compared with mEVs (Figure 1C), we focused on the effects induced by sEVs. E15.5 metatarsals were cultured in the following conditions: (a) basal medium (negative control), (b) osteogenic medium (positive control), (c) basal medium supplemented with 0.5 μg ADSC-sEVs, or (d) BMSC-sEVs. As shown in Figure 5A, at day 9 a mineralization center was observed only in the positive control. Bone growth was
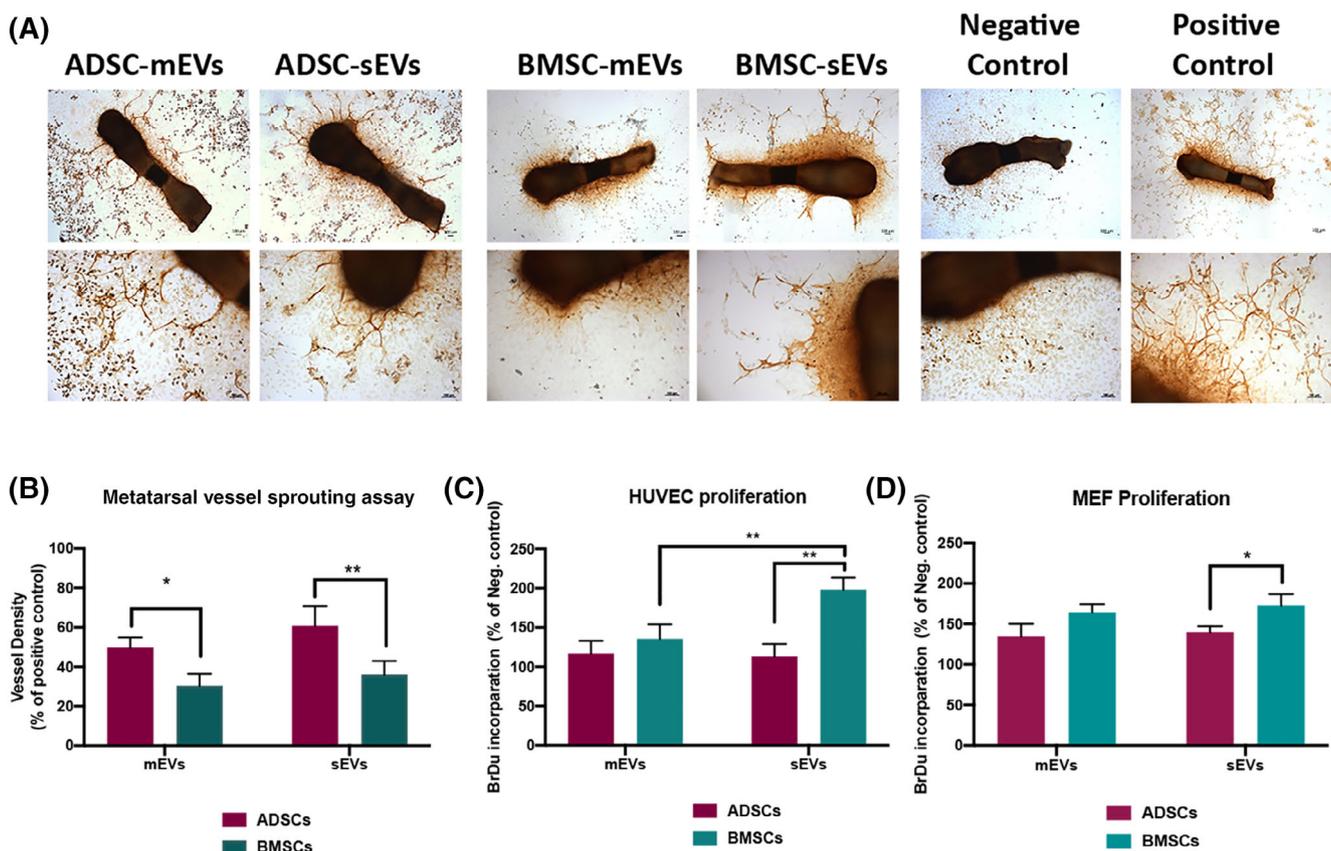
FIGURE 4 Ex vivo metatarsal sprouting assay. A, Representative image of CD31+ vessel structures, scale bar = 100 μm. B, Quantitative analysis of vessel density, CD31-positive cells were considered for the analysis. Quantitative analysis of BrDu incorporation (%) by HUVEC (C) and MEF (D). Data are presented as mean ± SD. N = 3, **$P < .01$, *$P < .05$, (two-way ANOVA and Tukey multiple comparison)

significantly higher in positive control compared with the other experimental groups ($P \leq .0001$) (Figure 5B). Although ADSC-sEVs seemed to promote metatarsal growth during the first 7 days in culture compared with both negative controls ($P = .0114$) and BMSC-counterparts ($P = .0220$) (Figure 5B), their effect appears to reach a *plateau* between day 7 and 9. This evidence suggests that, at macroscopic level, both ADSC- and BMSC-sEVs did not elicit drastic effects on metatarsal bone growth. For this reason, the pro-differentiative effect of EVs was further investigated at microscopic level, evaluating possible differences in the growth plate dynamics. Longitudinal bone growth occurs in the growth plate, in which chondrocytes are finely organized in resting, proliferative and hypertrophic zone.[27] As reported in Figure 6A, the resting zone (RZ) is characterized by single or paired chondrocytes,

irregularly dispersed and embedded in a cartilage matrix. Adjacent to the RZ, chondrocytes are flattened and arranged in columns parallel to the long bone axis. This proliferative zone (PZ) is the area of active cell replication, while the hypertrophic zone (HZ) is featured by enlarged, terminally differentiated cells and it initiates ossification by attracting vasculature.[27,28] Moreover, an intermediary zone termed prehypertrophic zone (pre-HZ) can lie between PZ and HZ.[29] Since it was not easy to discriminate precisely between pre-HZ and HZ, we will refer to pre-HZ/HZ in the description of the results associated to our experimental groups. We examined the morphology of chondrocytes within the growth plate and measured the extension of each zone, to understand the potential of MSC-sEVs in supporting EO. Negative controls exhibited a predominance of RZ (about 80% of total bone
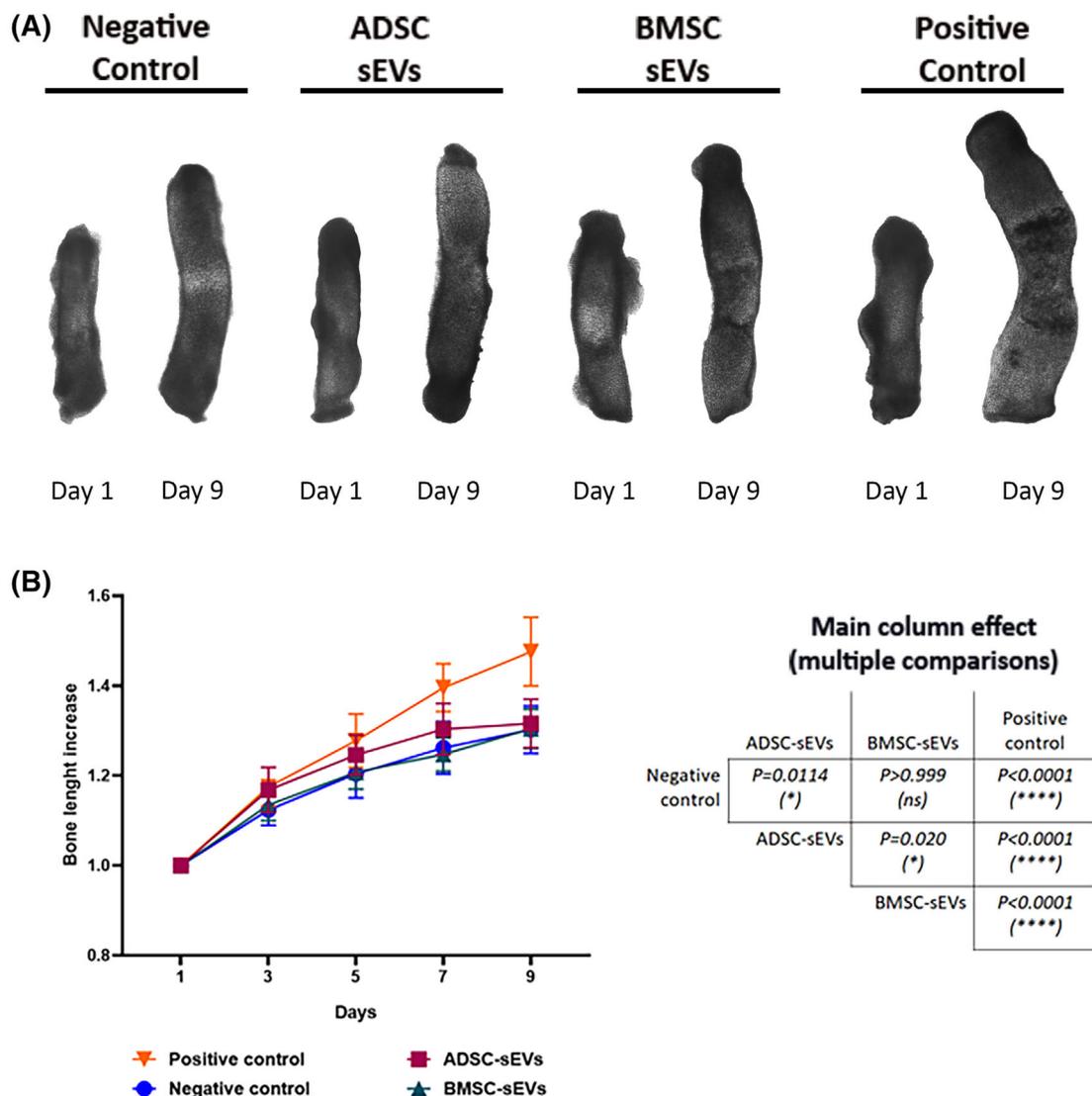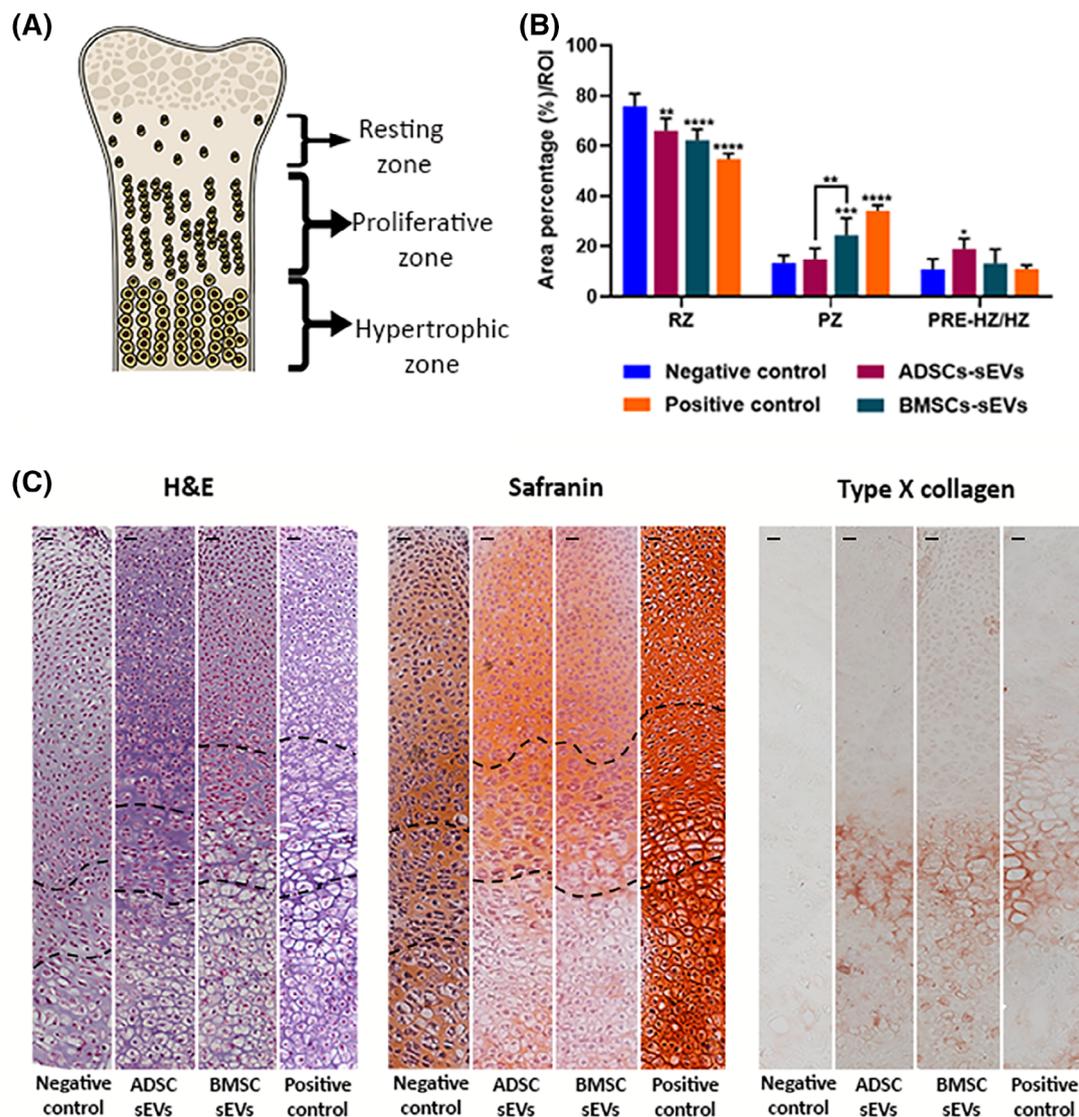

FIGURE 5 Effect of ADSC- and BMSC-derived sEVs on longitudinal bone growth. A, Representative images of mouse metatarsals at day 1 and day 9 of culture, in different culture conditions. B, Quantification of bone length increase during the time in different experimental groups. Each bone length was normalized on its day 1 value. Data are presented as mean ± SD. Table shows statistical significance between experimental groups. N = 10, ****$P < .0001$, *$P < .05$ (one-way ANOVA and Tukey multiple comparison)

area), while PZ represented a restricted flap, with a not well-organized structure, and pre-HZ/HZ was just sketchy (Figure 6B,C). Conversely, in positive controls all zones were clearly detectable (Figure 6C). RZ resulted strongly restricted compared with negative control ($P < .0001$), while PZ was abundant (about 40% of total bone area, $P > .0001$) (Figure 6A, B). No statistical differences were found in the extension of pre-HZ/HZ, even if positive control presented a more defined organization of the cells composing this area (Figure 6A,B). Similarly, both ADSC- and BMSC-sEVs induced a significant reduction of RZ compared with negative controls ($P < .01$ and $P < .0001$, respectively), but no statistical differences were observed between the two cell sources (Figure 6B). Interestingly, BMSC-sEVs triggered a significant increase in the PZ area

in comparison to both ADSC-sEVs and negative controls ($P < .01$ and $P < .001$, respectively). Accordingly, an initial columnar cell organization similar to positive control can be detected in the samples treated with BMSC-sEVs (Figure 6C).

No significant differences were noticed among ADSC- and BMSC-sEVs in pre-HZ/HZ area (Figure 6B). Type X-Collagen (Coll-X) is the main marker of hypertrophic chondrocytes.[30,31] Both EV-treated groups and positive controls expressed Coll-X in their pre-HZ/HZ, localized near the center, suggesting the establishment of a differentiation stage close to mineralization (Figure 6C). On the contrary, no Coll-X expression was detected in negative controls, confirming that in basal conditions bone metatarsal were stuck in a very early differentiation stage (Figure 6C).

FIGURE 6 Effect of ADSC- and BMSC-derived EVs on metatarsal growth plate organization. A, Schematic representation of growth plate morphology. B, Quantification of growth plate zones in different experimental groups. Area of the zone is calculated and reported as percentage of area/ROI (ROI = total bone area). Data are presented as mean ± SD. N = 5, (*) represent statistical significance compared with negative control. Statistics between ADSC- and BMSC-sEVs are also reported. ****$P < .0001$, ***$P < .001$, **$P < .01$, *$P < .05$ (two-way ANOVA and Tukey multiple comparison). C, Representative H&E, Safranin, and type-X collagen staining images of different groups. Scale bar = 100 μm
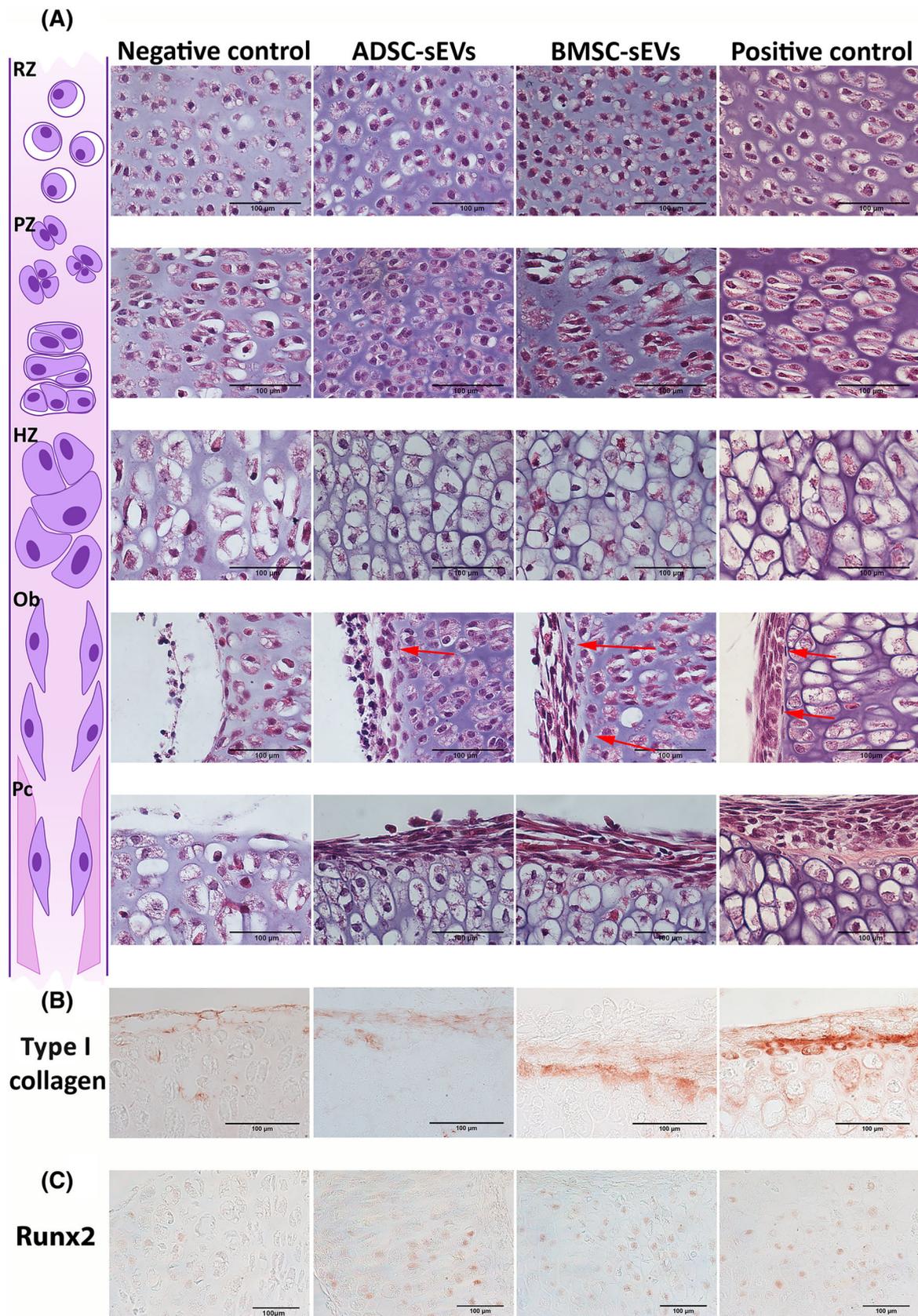
FIGURE 7 High magnification images of metatarsal bones. A, Representative H&E images of different zones at high magnification, to show details and chondrocytes morphology in different experimental groups. RZ, resting zone; PZ, proliferative zone; pre-HZ/HZ, pre-hypertrophic/hypertrophic zone; Ob, osteoblast-like cells; Pc, perichondrium. Red arrows indicated Ob. B, Type I collagen staining. C, Runx2 staining. Scale bar = 100 μm

Apart from the extension, also the morphology and spatial orientation of the cells composing each zone are responsible for the correct organization of the growth plate.[27] RZ was well distinguishable in all experimental groups and, as expected, it was characterized by single or paired chondrocytes immersed in a dense matrix (Figure 7A). In positive controls, PZ-chondrocytes were arranged in columns parallel to the long axis of the bone (Figure 7A), and pre-HZ/HZ were characterized by enlarged cells, with a matrix relegated to some portions surrounding the hypertrophic cells (Figure 7A). Close to the perichondrium, flattened and elongated cells with an osteoblast-like morphology were progressively incorporated in a bone-like matrix in the area straddling PZ and pre-HZ/HZ (Figure 7A). On the contrary, in negative controls, PZ-chondrocytes started to show their flattened morphology, but they were not able to self-orientate and arrange into columnar structures (Figure 7A). These cells enlarged in pre-HZ/HZ, but they were still scattered, and portions of dense cartilaginous matrix were still visible. No osteoblast-like cells were detectable, and perichondrium was not organized (Figure 7A).

Similarly to positive controls, the proliferative zone of BMSC-sEV-treated groups presented flattened and self-orientated chondrocytes starting to arrange into columns parallel to bone growth axis (Figure 7A). A different outcome was observed in ADSC-sEV groups, where proliferating chondrocytes were not able to organize in columns and remained chondron-like entities (Figure 7A). In both EV groups, hypertrophic chondrocytes of pre-HZ/HZ were enlarged and compacted, like positive controls. Close to perichondrium, few osteoblast-like cells were detectable in BMSC-sEV-treated metatarsals. Taken together, these observations suggest that BMSC-sEVs possess a more pronounced differentiation potential, promoting the correct spatial organization of the different growth plate area, particularly the proliferative zone. Finally, the expression of two specific markers, type I collagen (Coll I) and runt-related transcription factor 2 (Runx2), was also checked. Coll I was mainly expressed in positive control and, with less intensity, in BMSC-EVs-treated samples and it was found mostly around the osteoblast-like cells and in the elongated cells near pre-HZ/HZ (Figure 7B). Contrarily, ADSC-EVs showed a weaker expression of Coll I, while negative control had no Coll I positive cells (Figure 7B). Runx2 was found in positive controls, but also in ADSC-EVs and BMSC-EVs (Figure 7C).

4 | DISCUSSION

MSC-EVs have gained significant interest as cell-free regenerative therapies.[32] EVs are heterogeneous cell-derived membranous structures, originating from the endosomal compartment or shedding from plasma membrane.[13] Due to their biogenesis, the biological message transferred by EVs reflects the information carried by parental cells.[33] Indeed,

MSC-EVs have been reported to be effective in numerous preclinical models, recapping the cell-mediated effects.[34] In particular, they have been reported as novel cell-free alternatives to cell therapy with MSCs in the context of some bone-related pathologies, such as osteoarthritis (OA),[35] rheumatoid arthritis (RA),[36,37] osteoporosis (OP),[38,39] osteonecrosis,[40] and bone fracture.[41] Finally, MSC-EV therapy has the potential to become a novel cell-free therapy also for genetic disorders like osteogenesis imperfecta.[42] EVs can be easily isolated from MSCs of various origins, including AD and BM. Although both ADSC- and BMSC-derived EVs are indifferently used in many studies,[43] it is not yet clear whether and how the MSC source can affect EV structure and content and consequent biological function.

In this study, we isolated mEVs and sEVs from ADSCs and BMSCs and we compared their activity in a highly physiological ex vivo model of EO. Most of the vesicles released by both cell types were enriched in sEVs (100 K pellet). This could have a functional reason, since it has been reported that MSC-derived sEVs are therapeutically effective in different preclinical models.[44] However, once isolated, EV subpopulations from both cell sources exhibited similar characteristics. According to MISEV 2018 guidelines, ADSC- and BMSC-sEVs were enriched in syntenin, a cytosolic protein described to be segregated mostly in small vesicles, being involved in exosome biogenesis.[24] As expected, tetraspanins CD81 and CD63 were highly abundant in both sEVs, but CD81 was also present, to various degrees, in mEVs and in the corresponding cell lysates. CD9 was not detected in any of the EV populations analyzed, confirming its absence in MSC-derived vesicles.[24] Interestingly, flotillin-1, a caveolae associated factor, was the only protein whose expression differentiated EVs released by ADSCs and BMSCs, being expressed by both mEVs and sEVs secreted by ADSCs, but only by BMSC-mEVs.

A better understanding of how specific factors are sorted into EV subpopulations could help to elucidate their biological role. ADSC-mEVs were mainly enriched in factors involved in the response to damage, such as GRO-α and IL-8, two structurally related proteins with a potent neutrophil-stimulating activity,[45,46] IGFBP3, that modulates endothelial cell behavior and mediates cytoprotection following vascular injury,[47] and DKK-1, an antagonist of the Wnt/β-catenin signaling involved in tissue homeostasis and repair, whose expression is induced by inflammatory cytokines.[48] Conversely, biological factors involved in the modulation of angiogenic and osteogenic responses (ANG-2 and BDNF), as well as in the crosstalk with immune cells (IFN-γ, IL-1α, and KLK-3) were upregulated in BMSC-mEVs. Indeed, ANG-2 is a well-known growth factor belonging to the angiopoietin/TIE pro-angiogenic signaling pathway.[49] BDNF is a growth factor described to play a role in the modulation of bone repair increasing the expression of the osteogenic markers.[50] IFN-γ and IL-1α are two important immunomodulators that trigger MSCs towards an anti-inflammatory and pro-trophic phenotype.[51-53] KLK3 is an

angiogenesis suppressor.[54] Surprisingly, the pro-inflammatory adipokine RETN, described to regulate MSC proliferation and homing,[55,56] was significantly upregulated in BMSC-mEVs. PAI-1 was the only upregulated protein in ADSC-sEVs. PAI-1 exerts both pro- and anti-angiogenic properties, with the concentration of PAI-1 being an important determinant of which effect is observed.[57] On the other side, three proteins associated with MSC osteogenic differentiation (EMMPRin, uPAR, and HGF) were overexpressed by BMSC-sEVs. The glycoprotein EMMPRin (CD147), has been found to be upregulated in MSCs, and in particular in osteogenically-differentiated MSCs.[58] The multifunctional receptor uPAR mediates mobilization, migration and differentiation of MSCs, controlling their trafficking to the vascular wall in response to injury.[59] Finally, HGF promotes osteogenic differentiation through the expression of key osteogenic markers in human MSCs and it is a necessary component for the establishment of osteoblast mineralization.[60] The results described above suggest that EVs, and in particular sEVs, are enriched in proteins that could play a key role in angiogenesis and osteogenic differentiation, two fundamental phases of the EO process. For this reason, the fetal metatarsal bone explant model has been selected, since it recapitulates these phases, providing conditions closer to the in vivo situation than cells grown in monolayer or 3D culture.[21,26] Indeed, EO acts on three different levels: the differentiation of chondrocytes and their maturation, the establishment of a vascularized network that supports the ossification process, and the bone remodeling. Different studies demonstrated functional differences between BMSCs and ADSCs in this regard. BMSCs appear to be more osteoinductive than ADSCs in vivo. On the other hand, ADSCs contain vasculogenic subpopulations, which could be effective for bone repair, by promoting neovascularization. Accordingly, also their secretory profile can undergo variations dependent on the cell source. Hsiao and colleagues have already shown that ADSC total secretome exerts enhanced pro-angiogenic activities than BMSC-derived one.[61] In our study, we showed that the EV-encapsulated components of the ADSC secretome exhibit greater angiogenic capabilities compared with BMSC-counterparts, confirming that ADSCs could be preferred over other MSC populations in therapeutic approaches dependent upon angiogenesis. Nevertheless, the ability of EVs released by either ADSCs or BMSCs to interfere with the subsequent phases of EO is still unclear. Long bone growth occurs in the growth plate, a structure in which cartilage is clearly organized in three different horizontal layers: resting, proliferative and pre-hypertrophic/hypertrophic zone (RZ, PZ, pre-HZ/HZ), and the chondrocyte cell fate is recapitulated along the different areas. In RZ, chondrocytes start to replicate, and the daughter cells flatten and arrange themselves in columnar structures, orientated parallel to the growth axis. When chondrocytes stop replicating, they enlarge, reaching a terminally differentiated state. This peculiar organization and spatial orientation guides EO, leading to the maturation of cartilage and its remodeling into bone.[27,28] The ex vivo E15.5 bone explant model allowed us to evaluate the role played by ADSC- and BMSC-EVs on growth plate morphology. Although neither type of vesicle can induce significant macroscopic differences in terms of bone growth, BMSC-sEVs induced a more defined spatial organization of the growth plate, compared with ADSC-sEVs. The substantial difference lied in the organization of chondrocytes within the PZ, which is known to play a crucial role in EO, being the region of active cell replication. Columns in PZ are formed by four to eight flattened chondrocytes, longitudinally oriented. This orientation is related to a well-defined cartilage matrix composition, whose maturation determines an increase in matrix stiffness and drives the transition from round to flat chondrocytes.[62] The morphometric analysis of E15.5 metatarsals revealed that the percentage of PZ-area/total area was significantly increased in the BMSC-sEV treated groups compared with ADSC counterparts. The latter did not induce any change in PZ area compared with negative control. More importantly, PZ-chondrocytes of BMSC-sEV-treated groups maintained the flat columnar arrangement embedded in the extracellular matrix, which is not detected in ADSC-sEV and negative control groups. It is well known that the mechanisms of chondrocyte mediolateral elongation involve, among the others, several morphogenetic signals that modulate chondrocyte orientation.[62] Contrary to ADSC, BMSC-sEVs release signals that guide the spatial organization of chondrocytes in this specific and fundamental area of the growth plate that will dictate bone growth. Moreover, we provided evidence that initial perichondral formation occurred in positive controls, where a vis-à-vis cell pattern between elongated osteoblast-like cells (type I collagen positive) and hypertrophic chondrocytes (type x collagen and runx2 positive) was detected. Only in BMSC-sEV-treated metatarsals we could appreciate an initial collar organization with elongated cells placed in front of the hypertrophic chondrocytes as described by Riminucci and colleagues.[63] Despite our ex vivo E15.5 explant model is a powerful tool that closely mimics the in vivo process, it presents some drawbacks, such as limited lifespan and absence of a vascular network that could lead to a complete ossification of HZ-chondrocytes. This could partially explain the poor differences observed in pre-HZ/HZ of treated metatarsals, in the organization of perichondrium and the total bone length. Further investigations using ex vivo bone cultures derived from different developmental stages could help to better discriminate the EV-mediated effects and understand the priming of bone formation.

Various reports indicate that, regardless of the cell source, MSC-derived EVs possess immunomodulatory, pro-regenerative, pro-angiogenic and anti-apoptotic properties.

Nevertheless, few of them focus on the mechanism of action of MSC-EVs during embryonic tissue development, a key point to better understand tissue remodeling and regeneration. The intrinsic characteristics of EVs make them an

interesting strategy for tissue repair and regeneration. In this context, their use presents some advantages, but also some drawbacks. On one hand, EV structure protects their cargo, contributing to increase their ability to deliver the content into the cytosol of recipient cells. Moreover, EV-based strategies bypass the problems of immunogenicity and toxicity. However, there are still quite a few limitations to be addressed before EVs can be developed into a practical and effective therapeutic. Among these, the confusion regarding their precise biogenesis and the difficulties in tracking their fate after in vivo administration. Last, but not least, the related mechanisms of action are still at an early stage of comprehension and will require further investigation.

This study shows how the differences among MSC sources are reflected in the corresponding EVs, highlighting the importance of selecting the appropriate cell source for the development of innovative cell-free therapeutic strategies.

5 | CONCLUSION

This work explores the role of MSC-EVs during the differentiation and maturation of cartilage and points out how EVs from different origins can modulate early endochondral bone formation process in a different manner. Therefore, despite apparently few differences were found between EVs derived from ADSCs and BMSCs, a deeply investigation of their biological effects is crucial, before selecting the optimal EV-cell source.

CONFLICT OF INTEREST
The authors declared no potential conflicts of interest.

AUTHOR CONTRIBUTIONS
C. Gorgun and M.E.F.P.: conception and design, collection and/or assembly of data, data analysis and interpretation, manuscript writing, final approval of manuscript; D.R., M.C.G., K.C.: collection and/or assembly of data, data analysis and interpretation, final approval of manuscript; R.T. and C. Gentili: conception and design, financial support, manuscript writing, final approval of manuscript.

ORCID
Cansu Gorgun https://orcid.org/0000-0002-0460-2952
Maria Elisabetta Federica Palamà https://orcid.org/0000-0001-5585-137X
Chiara Gentili https://orcid.org/0000-0001-6745-3782

REFERENCES
1. Hoogduijn MJ, Lombardo E. Mesenchymal stromal cells anno 2019: dawn of the therapeutic era? Concise review. *Stem Cells Translational Medicine*. 2019;8:1126-1134.
2. da Silva ML, Chagastelles PC, Nardi NB. Mesenchymal stem cells reside in virtually all post-natal organs and tissues. *J Cell Sci*. 2006;119:2204-2213.
3. Nombela-Arrieta C, Ritz J, Silberstein LE. The elusive nature and function of mesenchymal stem cells. *Nat Rev Mol Cell Biol*. 2011;12:126-131.
4. Glenn JD. Mesenchymal stem cells: emerging mechanisms of immunomodulation and therapy. *World J Stem Cells*. 2014;6:526-539.
5. Laroye C, Gauthier M, Antonot H, Decot V, Reppel L, Bensoussan D. Mesenchymal stem/stromal cell production compliant with good manufacturing practice: comparison between bone marrow, the gold standard adult source, and Wharton's jelly, an extraembryonic source. *J Clin Med*. 2019;8:2207.
6. Mastrolia I, Foppiani EM, Murgia A, et al. Challenges in clinical development of mesenchymal stromal/stem cells: concise review. *Stem Cells Translational Medicine*. 2019;8:1135-1148.
7. Mazini L, Rochette L, Amine M, Malka G. Regenerative capacity of adipose derived stem cells (ADSCs), comparison with mesenchymal stem cells (MSCs). *Int J Mol Sci*. 2019;20(10):e2523.
8. Heo JS, Choi Y, Kim HS, et al. Comparison of molecular profiles of human mesenchymal stem cells derived from bone marrow, umbilical cord blood, placenta and adipose tissue. *Int J Mol Med*. 2016;37:115-125.
9. Fan XL, Zhang Y, Li X, Fu QL. Mechanisms underlying the protective effects of mesenchymal stem cell-based therapy. *Cell Mol Life Sci*. 2020;77:2771-2794.
10. Lu H, Wang F, Mei H, Wang S, Cheng L. Human adipose mesenchymal stem cells show more efficient angiogenesis promotion on endothelial colony-forming cells than umbilical cord and endometrium. *Stem Cells Int*. 2018;2018:1-15.
11. Baraniak PR, McDevitt TC. Stem cell paracrine actions and tissue regeneration. *Regen Med*. 2010;5:121-143.
12. Tetta C, Ghigo E, Silengo L, Deregibus MC, Camussi G. Extracellular vesicles as an emerging mechanism of cell-to-cell communication. *Endocrine*. 2013;44:11-19.
13. Yáñez-Mó M, Siljander PRM, Andreu Z, et al. Biological properties of extracellular vesicles and their physiological functions. *J Extracell Vesicles*. 2015;4:1-60.
14. Rani S, Ryan AE, Griffin MD, Ritter T. Mesenchymal stem cell-derived extracellular vesicles: toward cell-free therapeutic applications. *Mol Ther*. 2015;23:812-823.
15. Lo Sicco C, Reverberi D, Balbi C, et al. Mesenchymal stem cell-derived extracellular vesicles as mediators of anti-inflammatory effects: endorsement of macrophage polarization. *Stem Cells Translational Medicine*. 2017;6:1018-1028.

16. Van Deun J, Mestdagh P, Agostinis P, et al. EV-TRACK: transparent reporting and centralizing knowledge in extracellular vesicle research. *Nat Methods*. 2017;14(3):228-232.

17. Gorgun C, Ceresa D, Lesage R, et al. Dissecting the effects of preconditioning with inflammatory cytokines and hypoxia on the angiogenic potential of mesenchymal stromal cell (MSC)-derived soluble proteins and extracellular vesicles (EVs). *Biomaterials*. 2021;269:120633.

18. Palamà MEF, Shaw GM, Carluccio S, et al. The secretome derived from mesenchymal stromal cells cultured in a xeno-free medium promotes human cartilage recovery in vitro. *Front Bioeng Biotechnol*. 2020;8:e90.

19. Ludwig A-K, De Miroschedji K, Doeppner TR, et al. Precipitation with polyethylene glycol followed by washing and pelleting by ultracentrifugation enriches extracellular vesicles from tissue culture supernatants in small and large scales. *J Extracell Vesicles*. 2018;7:1528109.

20. Gorgun C, Reverberi D, Rotta G, Villa F, Quarto R, Tasso R. Isolation and flow cytometry characterization of extracellular-vesicle subpopulations derived from human mesenchymal stromal cells. *Curr Protoc Stem Cell Biol*. 2019;48:e76.

21. Song W, Fhu CW, Ang KH, et al. The fetal mouse metatarsal bone explant as a model of angiogenesis. *Nat Protoc*. 2015;10:1459-1473.

22. Dominici M, Le Blanc K, Mueller I, et al. Minimal criteria for defining multipotent mesenchymal stromal cells. The International Society for Cellular Therapy position statement. *Cytotherapy*. 2006;8:315-317.

23. Lin C-S, Ning H, Lin G, Lue TF. Is CD34 truly a negative marker for mesenchymal stromal cells? *Cytotherapy*. 2012;14:1159-1163.

24. Théry C, Witwer KW, Aikawa E, et al. Minimal information for studies of extracellular vesicles 2018 (MISEV2018): a position statement of the International Society for Extracellular Vesicles and update of the MISEV2014 guidelines. *J Extracell Vesicles*. 2018;7:1535750.

25. Kowal J, Arras G, Colombo M, et al. Proteomic comparison defines novel markers to characterize heterogeneous populations of extracellular vesicle subtypes. *Proc Natl Acad Sci USA*. 2016;113:E968-E977.

26. Houston DA, Staines KA, Macrae VE, et al. Culture of murine embryonic metatarsals: a physiological model of endochondral ossification. *J Vis Exp*. 2016;118:e54978.

27. Abad V, Meyers JL, Weise M, et al. The role of the resting zone in growth plate chondrogenesis. *Endocrinology*. 2002;143:1851-1857.

28. Hunziker EB. Mechanism of longitudinal bone growth and its regulation by growth plate chondrocytes. *Microsc Res Tech*. 1994;28:505-519.

29. Hallett SA, Ono W, Ono N. Growth plate chondrocytes: skeletal development, growth and beyond. *Int J Mol Sci*. 2019;20:e6009.

30. Reno PL, McBurney DL, Lovejoy CO, et al. Ossification of the mouse metatarsal: differentiation and proliferation in the presence/absence of a defined growth plate. *Anat Rec Pt A Discov Mol Cell Evol Biol*. 2006;288:104-118.

31. Shen G. The role of type X collagen in facilitating and regulating endochondral ossification of articular cartilage. *Orthod Craniofacial Res*. 2005;8:11-17.

32. Keshtkar S, Azarpira N, Ghahremani MH. Mesenchymal stem cell-derived extracellular vesicles: novel frontiers in regenerative medicine. *Stem Cell Res Ther*. 2018;9:63.

33. Zaborowski MP, Balaj L, Breakefield XO, et al. Extracellular vesicles: composition, biological relevance, and methods of study. *Bioscience*. 2015;65:783-797.

34. Maumus M, Rozier P, Boulestreau J, Jorgensen C, Noël D. Mesenchymal stem cell-derived extracellular vesicles: opportunities and challenges for clinical translation. *Front Bioeng Biotechnol*. 2020;8:997.

35. Tofiño-Vian M, Guillén MI, Del Caz MDP, et al. Microvesicles from human adipose tissue-derived mesenchymal stem cells as a new protective strategy in osteoarthritic chondrocytes. *Cell Physiol Biochem*. 2018;47:11-25.

36. Chen Z, Wang H, Xia Y, Yan F, Lu Y. Therapeutic potential of mesenchymal cell-derived miRNA-150-5p-expressing exosomes in rheumatoid arthritis mediated by the modulation of MMP14 and VEGF. *J Immunol*. 2018;201:2472-2482.

37. Cosenza S, Toupet K, Maumus M, et al. Mesenchymal stem cells-derived exosomes are more immunosuppressive than microparticles in inflammatory arthritis. *Theranostics*. 2018;8:1399-1410.

38. Qi X, Zhang J, Yuan H, et al. Exosomes secreted by human-induced pluripotent stem cell-derived mesenchymal stem cells repair critical-sized bone defects through enhanced angiogenesis and osteogenesis in osteoporotic rats. *Int J Biol Sci*. 2016;12:836-849.

39. Zuo R, Liu M, Wang Y, et al. BM-MSC-derived exosomes alleviate radiation-induced bone loss by restoring the function of recipient BM-MSCs and activating Wnt/β-catenin signaling. *Stem Cell Res Ther*. 2019;10:1-13.

40. Xian D, Shen L-H, Yi Z, et al. Exosomes from adipose-derived stem cells can prevent medication-related osteonecrosis of the jaw. *Med Sci Monit Int Med J Exp Clin Res*. 2021;27:e929684-1.

41. Furuta T, Miyaki S, Ishitobi H, et al. Mesenchymal stem cell-derived exosomes promote fracture healing in a mouse model. *Stem Cells Translational Medicine*. 2016;5:1620-1630.

42. Otsuru S, Desbourdes L, Guess AJ, et al. Extracellular vesicles released from mesenchymal stromal cells stimulate bone growth in osteogenesis imperfecta. *Cytotherapy*. 2018;20:62-73.

43. Martin-Rufino JD, Espinosa-Lara N, Osugui L, Sanchez-Guijo F. Targeting the immune system with mesenchymal stromal cell-derived extracellular vesicles: what is the Cargo's mechanism of action? *Front Bioeng Biotechnol*. 2019;7:e308.

44. Witwer KW, Van Balkom BWM, Bruno S, et al. Defining mesenchymal stromal cell (MSC)-derived small extracellular vesicles for therapeutic applications. *J Extracell Vesicles*. 2019;8:1609206.

45. Geiser T, Dewald B, Ehrengruber MU, Clark-Lewis I, Baggiolini M. The interleukin-8-related chemotactic cytokines GROα, GROβ, and GROγ activate human neutrophil and basophil leukocytes. *J Biol Chem*. 1993;268:15419-15424.

46. Fujiwara K, Matsukawa A, Ohkawara S, Takagi K, Yoshinaga M. Functional distinction between CXC chemokines, interleukin-8 (IL-8), and growth related oncogene (GRO)α in neutrophil infiltration. *Lab Invest*. 2002;82:15-23.

47. Kielczewski JL, Jarajapu YPR, McFarland EL, et al. Insulin-like growth factor binding protein-3 mediates vascular repair by enhancing nitric oxide generation. *Circ Res*. 2009;105:897-905.

48. Koch S, Nava P, Addis C, et al. The Wnt antagonist Dkk1 regulates intestinal epithelial homeostasis and wound repair. *Gastroenterology*. 2011;141:259-268.e8.

49. Maisonpierre PC, Suri C, Jones PF, et al. Angiopoietin-2, a natural antagonist for Tie2 that disrupts in vivo angiogenesis. *Science (80-)*. 1997;277:55-60.

50. Loy TL, Vehlow D, Kauschke V, Müller M, Heiss C, Lips KS. Effects of BDNF and PEC nanoparticles on osteocytes. *Molecules*. 2020;25:4151.

51. Krampera M, Cosmi L, Angeli R, et al. Role for interferon-γ in the immunomodulatory activity of human bone marrow mesenchymal stem cells. *Stem Cells*. 2006;24:386-398.

52. Bodo M, Venti G, Pezzetti F, et al. Interleukin-1 alpha: regulation of cellular proliferation and collagen synthesis in cultured human osteoblast-like cells. *Cell Mol Biol (Noisy-le-Grand)*. 1992;38:679-686.

53. Redondo-Castro E, Cunningham C, Miller J, et al. Interleukin-1 primes human mesenchymal stem cells towards an anti-inflammatory and pro-trophic phenotype in vitro. *Stem Cell Res Ther*. 2017;8:79.

54. Fortier AH, Holaday JW, Liang H, et al. Recombinant prostate specific antigen inhibits angiogenesis in vitro and in vivo. *Prostate*. 2003;56:212-219.

55. Acquarone E, Monacelli F, Borghi R, Nencioni A, Odetti P. Resistin: a reappraisal. *Mech Ageing Dev*. 2019;178:46-63.

56. He Y, Guo Y, Xia Y, et al. Resistin promotes cardiac homing of mesenchymal stem cells and functional recovery after myocardial ischemia-reperfusion via the ERK1/2-MMP-9 pathway. *Am J Physiol Hear Circ Physiol*. 2019;316:H233-H244.

57. Wu J, Strawn TL, Luo M, et al. Plasminogen activator inhibitor-1 inhibits angiogenic signaling by uncoupling vascular endothelial growth factor receptor-2-αVβ3 integrin cross talk. *Arterioscler Thromb Vasc Biol*. 2015;35:111-120.

58. Chen J, Shi ZD, Ji X, et al. Enhanced osteogenesis of human mesenchymal stem cells by periodic heat shock in self-assembling peptide hydrogel. *Tissue Eng Pt A*. 2013;19:716-728.

59. Vallabhaneni KC, Tkachuk S, Kiyan Y, et al. Urokinase receptor mediates mobilization, migration, and differentiation of mesenchymal stem cells. *Cardiovasc Res*. 2011;90:113-121.

60. Aenlle KK, Curtis KM, Roos BA, Howard GA. Hepatocyte growth factor and p38 promote osteogenic differentiation of human mesenchymal stem cells. *Mol Endocrinol*. 2014;28:722-730.

61. Hsiao ST-F, Asgari A, Lokmic Z, et al. Comparative analysis of paracrine factor expression in human adult mesenchymal stem cells derived from bone marrow, adipose, and dermal tissue. *Stem Cells Dev*. 2012;21:2189-2203.

62. Prein C, Warmbold N, Farkas Z, Schieker M, Aszodi A, Clausen-Schaumann H. Structural and mechanical properties of the proliferative zone of the developing murine growth plate cartilage assessed by atomic force microscopy. *Matrix Biol*. 2016;50:1-15.

63. Riminucci M, Bradbeer JN, Corsi A, et al. Vis-a-vis cells and the priming of bone formation. *J Bone Miner Res*. 1998;13:1852-1861.